

- dysz, J. A.; Academic Press, 1, 1982.
20. P. M. Treichel and R. L. Shubkin, *Inorg. Chem.* **6**, 1328 (1967).
21. R. H. Crabtree, *The Organometallic Chemistry of the Transition Metals*, John Wiley, 280, 1988.
22. *Handbook of Chemistry and Physics*, 55 th ed.: CRC; Cleveland, OH, 1974/1975; PF-198.
23. Y. Kim and K. Seff, *J. Phys. Chem.* **82**, 1307 (1978).
24. Y. Kim and K. Seff, *J. Phys. Chem.* **82**, 921 (1978).
25. Y. Kim, S. H. Song, J. Y. Park, and U. S. Kim, *Bull. Korean Chem. Soc.*, **6**, 338 (1988).
26. Y. Kim and K. Seff, *J. Phys. Chem.* **82**, 1071 (1978).

Crystal Structure of Dehydrated Partially Ag⁺-Exchanged Zeolite A treated with Cesium Vapor at 250°C

Duk Soo Kim, Seong Hwan Song¹, and Yang Kim^{1*}

¹Department of Chemistry Cheju National University, Cheju 690-756

²Department of Chemistry Pusan National University, Pusan 609-735. Received December 23, 1988

The crystal structure of partially Ag⁺-exchanged zeolite A, Ag_{3.2}Na_{8.8}-A, vacuum dehydrated at 360 °C and then exposed to 0.1 torr of cesium vapor for 12 hours at 250 °C has been determined by single-crystal X-ray diffraction techniques in the cubic space group *Pm3m* (*a* = 12.262(2) Å) at 21(1) °C. The structure was refined to the final error indexes *R*₁ = 0.068 and *R*₂ = 0.072 by using 338 reflections for which *I*_o > 3σ(*I*_o) and the composition of unit cell is Ag_{3.2}Cs_{8.8}-A. 3 Cs⁺ ions lie on the centers of the 8-rings at sites of *D*_{4h} symmetry. Two crystallographically different 6-ring Cs⁺ ions were found: 1.5 Cs⁺ ions at Cs(2) are located inside of sodalite cavity and 4.3 Cs⁺ ions at Cs(3) are located in the large cavity. The fractional occupancies observed at Cs(2) and Cs(3) indicate that the existence of at least three types of unit cells with regard to the 6-ring Cs⁺ ions. For example, 50% of unit cells may have two Cs⁺ ions at Cs(2) and 4 Cs⁺ ions at Cs(3). 30% of unit cells may have one Cs⁺ ion at Cs(2) and 5 Cs⁺ ions at Cs(3). The remaining 20% would have one Cs⁺ ion at Cs(2) and 4 Cs⁺ ions at Cs(3). On threefold axes of the unit cell two non-equivalent Ag atom positions are found in the large cavity, each containing 0.64 and 1.92 Ag atoms, respectively. A crystallographic analysis may be interpreted to indicate that 0.64 (Ag₆)⁺ clusters are present in each large cavity. This cluster may be viewed as a tetrasilver molecule (Ag₄)⁰ (bond length, 2.84 Å) stabilized by the coordination of one Ag⁺ ion.

Introduction

Numerous investigation have been reported that various types of silver clusters are located in dehydrated fully and partially silver ion exchanged zeolite A, zeolite Y, mordenite, and chabazite.¹⁻¹⁰ The existence of these silver clusters was identified and reconfirmed by many workers using EPR spectroscopy,^{6,11-14} reflectance spectroscopy,¹⁵ and FTIR.¹⁶ Ag⁺ ions can be reduced by heating, by reaction with reducing agents such as H₂, alcohol, and alkylbenzenes, or by the sorption of metal atoms.¹⁷ Recently, in the structures of dehydrated Ag₆Na₆-A^{18,19} treated with 50 torr of H₂ at room temperature, 1.27 (Ag₃)⁺ clusters and 0.7 (Ag₃)²⁺ clusters per unit cell were found in the large cavity. In the structure of Ag_{4.6}Na_{7.4}-A, dehydrated and treated with H₂ at 350 °C, (Ag₆)³⁺ clusters of low symmetry were found in the large cavity.^{3,9}

In the structure of fully Cs⁺ ion exchanged zeolite A which was prepared by the sorption of cesium metal vapor on dehydrated Na₁₂-A, Na⁺ ions were reduced and replaced by Cs vapor and linear cesium clusters (Cs₃)²⁺ and (Cs₄)³⁺, were found.²⁰

This work was done to learn whether new silver clusters, or known clusters with unknown structure, could be synthesized for the reaction of Ag_{3.2}Na_{8.8}-A with cesium metal vapor as a reducing agent and, if so determine their structures by single-crystal X-ray diffraction techniques.

Experimental

Complete Ag⁺ exchange of zeolite 4A single crystals is accomplished by a static method. 0.2g of zeolite 4A (Union Carbide, Lot 494107701161) were allowed to exchange at 24°C with 6-fold excess of 0.05N AgNO₃, and the solution was agitated periodically. Each day, the supernatant solution was decanted and a fresh aliquot of 0.05N AgNO₃ was added. After 7 days, the zeolite was filtered and dried.

To prepare of Ag₄Na₈-A, samples of Ag₁₂-A and Na₁₂-A were mixed in a 3:1 mole ratio (neglecting water content). To this mixture was added a few large single crystals of zeolite 4A which had been prepared by Charnell's method,²⁰ with enough water to submerge all solid particles so that at equilibrium the composition of the large crystals would be Ag₄Na₈-A. After 4 days, the water was allowed to evaporate in air at room temperature.

A single crystal 80 μm on an edge was selected and lodged in a fine glass capillary. The hydrated partially Ag⁺-exchanged crystal was dehydrated for 48h at 360 °C and 2.0 × 10⁻⁶ torr, and then exposed to 0.1 torr of cesium vapor for 12h at 250 °C. After cooling to room temperature, the crystal was sealed off in its capillary by torch. The crystal became metallic black.

Diffraction intensities were subsequently collected at 21(1) °C. The space group *Pm3m* (no systematic absences) was used throughout this work for reasons discussed pre-

Table 1. Positional, Thermal^a, and Occupancy parameters of Dehydrated $Ag_{3.2}Cs_{8.8}A$

Atom	Wyc. Pos.	<i>x</i>	<i>y</i>	<i>z</i>	β_{11}	β_{22}	β_{33}	β_{12}	β_{13}	β_{23}	^b Occupancy varied fixed
(Si,Al)	24(<i>k</i>)	0	1837(2)	3709(2)	22(2)	18(2)	12(2)	0	0	9(3)	^c 24.0
O(1)	12(<i>h</i>)	0	2240(10)	5000	100(10)	35(9)	16(7)	0	0	0	12.0
O(2)	12(<i>i</i>)	0	2953(6)	2953(6)	46(8)	22(4)	22(4)	0	0	30(10)	12.0
O(3)	24(<i>m</i>)	1115(5)	1115(5)	3413(7)	30(3)	30(3)	63(7)	39(9)	11(8)	11(8)	24.0
Cs(1)	3(<i>c</i>)	0	5000	5000	162(4)	63(2)	63(2)	0	0	0	2.8(1)
Cs(2)	8(<i>g</i>)	913(7)	913(7)	913(7)	137(6)	137(6)	137(6)	-70(10)	-70(10)	-70(10)	1.43(3)
Cs(3)	8(<i>g</i>)	2805(2)	2805(2)	2805(2)	57(1)	57(1)	57(1)	11(3)	11(3)	11(3)	4.27(2)
Ag(1)	8(<i>g</i>)	2140(10)	2140(10)	2140(10)	41(6)	41(6)	41(6)	10(20)	10(20)	10(20)	0.75(4)
Ag(2)	12(<i>j</i>)	2420(5)	2420(5)	5000	300(30)	300(30)	60(30)	510(60)	0	0	0.45(4)
Ag(3)	8(<i>g</i>)	3840(10)	3840(10)	3840(10)	300(10)	300(10)	300(10)	80(40)	80(40)	80(40)	1.87(5)

^aPositional and isotropic thermal parameters are given $\times 10^4$. Numbers in parentheses are the esd's in units of the least significant digit given for the corresponding parameter. The anisotropic temperature factor = $\exp[-(\beta_{11}h^2 + \beta_{22}k^2 + \beta_{33}l^2 + \beta_{12}hk + \beta_{13}hl + \beta_{23}kl)]$. ^bOccupancy factors given as the number of atoms or ions per unit cell. ^cOccupancy for (Si) = 12; occupancy for (Al) = 12.

viously.^{21,22} Preliminary crystallographic experiments and subsequent data collection were performed with an Enraf-Nonius four-circle computer controlled CAD-4 diffractometer, equipped with scintillation counter, pulse-height analyzer, a PDP micro 11/73 computer, and a graphite monochromator. Molybdenum radiation ($K_{\alpha 1}$, $\lambda = 0.70930 \text{ \AA}$; $K_{\alpha 2}$, $\lambda = 0.71359 \text{ \AA}$) was used for all experiments. The unit cell constant, as determined by a least-squares refinements of 25 intense reflections for which $16^\circ < 2\theta < 25^\circ$ is $12.262(2) \text{ \AA}$.

Reflections from two intensity-equivalent regions of reciprocal space (hkl , $h \leq k \leq l$ and hkl , $k \leq h \leq l$) were examined using the ω - 2θ scan speeds. The maximum final scan speed was 5 min per one reflection. Most reflections were observed at the slow scan speed, ranging between 0.150° and 0.260° in $\omega \text{ min}^{-1}$. The intensities of three reflections in diverse regions of reciprocal space were recorded after every 100 reflections to monitor crystal and instrument stability. The raw data from each region were corrected for Lorentz and polarization effects, including that due to incident beam monochromatization; the reduced intensities were merged and resultant estimated standard deviation were assigned to each average reflection by computer programs PAINT and WEIGHT.²³ An absorption correction was judged to be unimportant ($\mu = 5.59 \text{ mm}^{-1}$) and was not applied.⁸ All 874 reflections for which $2\theta < 70^\circ$ were collected by counter methods. Of these, only the 338 for which $I_o > 3\sigma(I_o)$ were used for subsequent structure solution and refinement.

Structure Determination

Full-matrix least-squares refinement was initiated by using the atomic parameters of the framework atoms ((Si, Al), O(1), O(2), and O(3)) in the structure of the dehydrated $Ag_{4.6}Na_{7.4}A$.³ Anisotropic refinement converged to error indices,

$$R_1 = \sum |F_o - |F_c|| / \sum F_o = 0.554$$

$$R_2 = [\sum w(F_o - |F_c|)^2 / \sum wF_o^2]^{1/2} = 0.597$$

A difference Fourier map revealed two large peaks at (0.0, 0.5, 0.5) and (0.277, 0.277, 0.277) with heights of $35.4(5) \text{ e \AA}^{-3}$ and $23.7(3) \text{ e \AA}^{-3}$, respectively. These were stable in

least-squares refinement and anisotropic refinement including these positions, as Cs(1) and Cs(3), respectively, converged to $R_1 = 0.167$ and $R_2 = 0.243$. A subsequently difference Fourier map revealed four peaks at (0.082, 0.082, 0.082), (0.2207, 0.2207, 0.2207), (0.3887, 0.3887, 0.3887), and (0.2207, 0.2207, 0.5) with heights of $9.9(3) \text{ e \AA}^{-3}$, $9.2(3) \text{ e \AA}^{-3}$, $3.2(3) \text{ e \AA}^{-3}$, and $5.5(2) \text{ e \AA}^{-3}$, respectively. All of which were stable in least-squares refinement and simultaneous positional, occupancy, and anisotropic thermal parameter refinement including these positions, Cs(2), Ag(1), Ag(2), and Ag(3), respectively, converged to $R_1 = 0.062$ and $R_2 = 0.072$. At this point, a difference Fourier map revealed a peak at (0.359, 0.359, 0.359) with a height of $1.0(2) \text{ e \AA}^{-3}$. Unfortunately, attempt to refine this position as Ag(5) was unsuccessful. In least-squares refinement, this position was shifted to Ag(3) position. The error indices were also increased.

Occupancy refinements of Cs(1), Cs(2), Cs(3), Ag(1), Ag(2), and Ag(3) converged to 2.8(1), 1.43(3), 4.27(2), 0.75(4), 0.45(4), and 1.87(5), respectively (see Table 1). The ions at Cs(1) are associated with 8-rings, and because these ions can accommodate no more than 3 ions per unit cell, the occupancy at Cs(1) was fixed at 3. It appeared that the occupancy numbers of Ag(1) and Ag(2) were one third those of Ag(3). The Ag(1)-Ag(2) and Ag(1)-Ag(3) distances were $3.544(4) \text{ \AA}$ and $3.617(7) \text{ \AA}$, respectively. The approach distance of Ag(1) and Ag(2) to the framework oxide ion O(3) are $2.365(6) \text{ \AA}$ and $2.990(30) \text{ \AA}$, respectively, and that of Ag(2) to the framework oxide ion O(1) is $2.980(40) \text{ \AA}$. The Ag(2)-Ag(3) and Ag(3)-Ag(3) distances are $2.840(40) \text{ \AA}$ and $2.840(20) \text{ \AA}$, respectively. These distances indicate that Ag(2) and Ag(3) are occupied by silver atoms and Ag(1) is occupied by silver ion. They appear to form $(Ag_3)^+$ clusters (Figure 2). Therefore, the occupancy numbers of Ag(1), Ag(2), and Ag(3) was fixed to 0.64, 0.64, and 1.92. Therefore, the composition of unit cell is $Ag_{3.2}Cs_{8.8}A$ ($D_{cal} = 2.65 \text{ g cm}^{-3}$ and $F(000) = 1243$). The final refinements, using anisotropic thermal parameters for all positions, converged at $R_1 = 0.068$ and $R_2 = 0.072$.

The final difference map was featureless except for two peaks at the center of the unit cell and (0.359, 0.359, 0.359) with heights of $2.7(7) \text{ e \AA}^{-3}$, respectively.

The final structure parameters are presented in Table 1. Interatomic distances and angles are given in Table 2. All

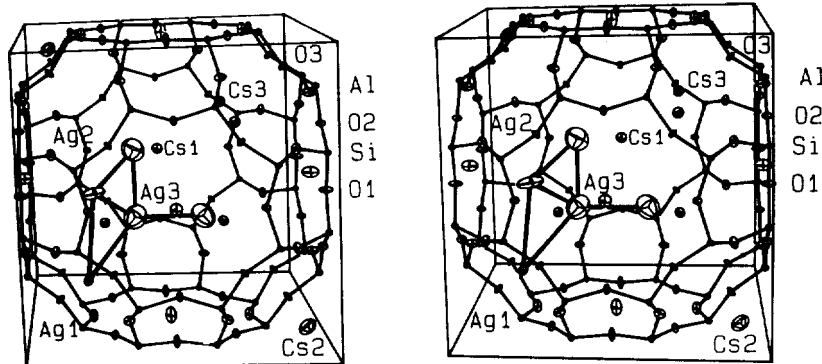


Figure 1. Stereoview of the structure showing one $(Ag_5)^+$ cluster per unit cell. About 64% of the unit cells contain this cluster and the remaining 36% would have no cluster.

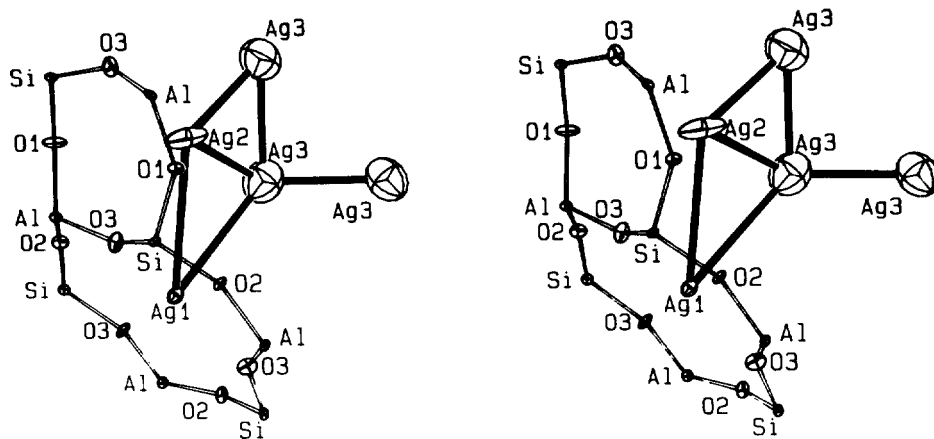


Figure 2. Stereoview of the $(Ag_5)^+$ cluster. The torsion angle of $Ag(2)-Ag(3)-Ag(3)-Ag(3)$ is 142.8° .

Table 2. Selected Interatomic Distances(Å) and Angles(deg)^a of Dehydrated $Ag_{3.2}Cs_{8.8}A$

(Si,Al)-O(1)	1.658(3)	O(1)-(Si,Al)-O(2)	106.9(3)
(Si,Al)-O(2)	1.653(3)	O(1)-(Si,Al)-O(3)	111.4(3)
(Si,Al)-O(3)	1.669(4)	O(2)-(Si,Al)-O(3)	108.6(1)
Ag(1)-O(3)	2.365(6)	O(3)-(Si,Al)-O(3)	110.1(3)
Ag(2)-O(1)	2.980(40)	(Si,Al)-O(1)-(Si,Al)	145.7(5)
Ag(2)-O(3)	2.990(30)	(Si,Al)-O(2)-(Si,Al)	158.1(3)
Cs(1)-O(1)	3.389(7)	(Si,Al)-O(3)-(Si,Al)	145.3(3)
Cs(1)-O(2)	3.550(30)	O(3)-Cs(2)-O(3)	80.4(1)
Cs(2)-O(2)	3.712(3)	O(3)-Cs(3)-O(3)	82.4(1)
Cs(2)-O(3)	3.086(7)	O(3)-Ag(1)-O(3)	114.8(3)
Cs(3)-O(2)	3.449(1)	O(1)-Ag(2)-O(2)	54.8(6)
Cs(3)-O(3)	3.025(3)	Ag(2)-Ag(3)-Ag(3)	60.0(3)
Cs(1)-Cs(3)	5.131(1)	Ag(1)-Ag(3)-Ag(3)	125.3(2)
Cs(3)-Cs(3)	5.384(1)	Ag(1)-Ag(2)-Ag(3)	68.0(2)
Cs(2)-Cs(3)	4.019(3)	Ag(2)-Ag(1)-Ag(3)	46.7(4)
Cs(2)-Cs(2)	3.877(6)		
Ag(1)-Ag(2)	3.544(4)		
Ag(1)-Ag(3)	3.617(7)		
Ag(2)-Ag(3)	2.840(40)		
Ag(3)-Ag(3)	2.840(20)		

^aNumbers in parentheses are estimated standard deviations in the units of the last significant digit given for the corresponding value.

shifts in the final cycle of refinement were less than 0.3% of their corresponding esd's.

The full-matrix least-squares program used in all struc-

Table 3. Deviation of Atoms(Å) from the (111) Plane at O(3) of Dehydrated $Ag_{3.2}Cs_{8.8}A$

O(2)	0.187(4)	Cs(2)	-2.057(5)
Cs(3)	1.963(1)	Ag(1)	0.546(8)
Ag(3)	4.164(9)		

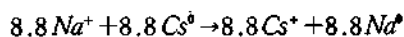
A negative deviation indicates that the atom lies on the same side of the planes as the origin.

ture determination minimized $\sum w(F_o - |F_c|)^2$; the weight(w) of an observation was the reciprocal squares of $\sigma(F_o)$, its standard deviation. Atomic scattering factors^{24,25} for Ag^0 , Ag^+ , O^- , Cs^+ , and $(Si,Al)^{1.75+}$ were used. The function describing $(Si,Al)^{1.75+}$ is the mean of the Si^0 , Si^{4+} , Al^0 , Al^{3+} functions. All scattering factors were modified to account for the anomalous dispersion correction.^{26,27}

Discussion

Cs^+ ions are found at three crystallographic sites, as presented in Table 1. In this structure three Cs^+ ions at Cs(1) fill the equipoints at the centers of the 8-rings.²⁸ These positions are well established by previous experimental works^{18,29,30} as well as by theoretical calculations.^{31,32} The local symmetry of this site is $C_{4h}(D_{4h}$ in $Pm3m$). Each Cs^+ ion is 3.389(7)Å from four O(1) oxygens and 3.550(30)Å from four O(2)'s. These distances are substantially large than the sum of ionic radii, 2.99Å³³, but Cs^+ ions at this position have also been observed before in the Cs^+ ion exchanged zeolite A structures.^{18,29,34-36} The Cs^+ ions at Cs(2) and Cs(3) are on three-fold axes and associated with 6-rings.²⁸ The 1.5 ions at Cs(2)

are recessed 2.057(5)Å into the sodalite cavity from the (111) plane at O(3), and the 4.3 ions at Cs(3) are correspondingly recessed 1.963(1)Å into the large cavity (see Table 3). These ions are each associated with three O(3) oxygens, at 3.086(7)Å for Cs(2) and 3.025(3)Å for Cs(3) (see Table 2). In this crystal structure, Na^+ ions were reduced by cesium metal vapor and replaced by Cs^+ ions.³¹ This reaction is driven by the following equation:



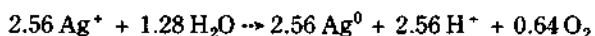
This can be considered a solvent-free ion exchange method.

The fractional occupancies observed at Cs(2) and Cs(3) indicate that the existence of at least three types of unit cells with regard to the 6-ring Cs^+ ions. For example, 50% of unit cells may have two Cs^+ ions at Cs(2) and 4 Cs^+ ions at Cs(3). 30% of unit cells may have one Cs^+ ion at Cs(2) and 5 Cs^+ ions at Cs(3). The remaining 20% would have one Cs^+ ion at Cs(2) and 4 Cs^+ ions at Cs(3).

The silver species at Ag(1) are located near framework oxygens and may be considered to be Ag^+ ions. Ag(1) is associated with a six-ring and approaches three O(3) oxygens at 2.365(6)Å. For comparison, the sum of the Ag^+ and O^{2-} radii is 2.58Å.³⁷

The silver species at Ag(3) are located deep inside the large cavity. The distance between Ag(3) and O(3) is 4.760(50)Å, indicating that there is no interaction between silver species at Ag(3) and O(3) oxygen. They may be placed within their equipoints of partial occupancy: $Ag(3)-Ag(3) = 2.840(20)Å$ (see Table 2). This distance is approximately the same as the Ag^0-Ag^0 distance in silver metal, 2.89Å.³⁶ An $Ag(1)-Ag(3)$ distance is 3.617(7)Å (Table 2) which is too short to be an unmoderated Ag^+-Ag^+ contact and too long to be Ag^0-Ag^0 bond. This may be considered to be Ag^0-Ag^+ coordination distance.^{1,2}

The Ag(2) position is 2.980(40)Å and 2.990(30)Å from two O(1) oxygens and two O(3) oxygen, respectively. $Ag(1)-Ag(2)$ and $Ag(3)-Ag(2)$ distances are 3.544(4)Å and 2.840(40)Å (see Table 2), respectively, indicating that $Ag(1)-Ag(2)$ is an ion-atom contact and $Ag(3)-Ag(2)$ is an atom-atom contact. Therefore, Ag(2) is a silver atom position. However, $Ag(1)-Ag(2)$ and $Ag(1)-Ag(3)$ distances as a distance of Ag^+ ion and Ag atom are longer than those of $(Ag_6)^+(Ag_6^0)$ in the structure of dehydrated partially decomposed $Ag_{12}A$.^{1,2} The anisotropic thermal ellipsoids at Ag(2) and Ag(3) are relatively large, indicating that those atoms are less firmly positioned. Thus, the Ag^+-Ag^0 distances in this structure are elongated. Such elongated Ag^+-Ag^0 distance is also seen at the structure of $(Ag_3)^{2+}$ clusters in Ag_6Na_6A .⁹ The reduction of Ag^+ to Ag^0 per unit cell may be proceeded by following reaction.



The number of silver ions or atoms at Ag(1), Ag(2), and Ag(3) are 0.64, 0.64, and 1.92, respectively (Table 1). This suggests that 0.64 cluster with stoichiometry 1:1:3 has formed per unit cell. This cluster is $(Ag_6)^+$ as shown in Figure 2.

The composition of the crystal could not have been Ag_4Na_8A , as was intended, before treatment with cesium vapor. This could have been due to our neglect of zeolitic water molecules in calculating the weight ratio of hydrated

$Na_{12}A$ and $Ag_{12}A$ to be mixed in the preparation step. One reason for this neglect is that the water content of hydrated $Ag_{12}A$ is not accurately known. It is also possible that the single crystal studied was not in proper equilibrium with bulk sample.

Acknowledgements. This work was supported by the Korean Science and Engineering Foundation.

References

1. Y. Kim and K. Seff, *J. Am. Chem. Soc.*, **99**, 7055 (1977).
2. Y. Kim and K. Seff, *J. Am. Chem. Soc.*, **100**, 6989 (1978).
3. Y. Kim and K. Seff, *J. Phys. Chem.*, **91**, 668 (1987).
4. Y. Kim and K. Seff, *J. Phys. Chem.*, **91**, 671 (1987).
5. H. Tsutsumi and H. Takahashi, *Bull. Chem. Soc. Jpn.*, **45**, 2332 (1972).
6. H. K. Beyer and P. A. Jacobs, in "Metal Microstructures in Zeolites"; P. A. Jacobs, Ed.; Elsevier Scientific; Amsterdam, 1982, pp. 95-102.
7. H. K. Beyer, P. A. Jacobs, and J. B. Uytterhoeven, *J. Chem. Soc., Faraday Trans. I*, **72**, 674 (1976).
8. Y. Kim and K. Seff, *J. Phys. Chem.*, **82**, 925 (1978).
9. Y. Kim and K. Seff, *Bull. Korean Chem. Soc.*, **5**, 135 (1984).
10. D. S. Kim, S. H. Song and Y. Kim, *Bull. Korean Chem. Soc.*, **9**, 303 (1988).
11. D. Hermerschmidt and R. Haul, *Ber. Bunsenges Phys. Chem.*, **84**, 902 (1980).
12. P. J. Grobet and R. A. Schoonheydt, *Surf. Sci.*, **156**, 893 (1985).
13. G. A. Ozin, F. Hugues, S. Mattar, and D. McIntosh, Presented at the 184th National Meeting of the American Chemical Society, New York, Sept., 1982; INCR71.
14. J. R. Morton K. P. Preston, *J. Magn. Reson.*, **68**, 121 (1986).
15. L. R. Gellens and R. A. Schoonheydt, in "Metal Microstructures in Zeolites"; P. A. Jacobs, Ed.; Elsevier Scientific; Amsterdam, 1982; pp. 87-94.
16. G. A. Ozin, M. D. Baker and J. J. Godber, *J. Phys. Chem.*, **88**, 4902 (1984).
17. L. B. McCuster, Ph. D. Thesis, University of Hawaii, 1980.
18. The nomenclature refers to the contents of the $Pm3m$ unit cell. For example, Ag_6Na_6A represents $Ag_6Na_6Si_{12}Al_{12}O_{48}$, exclusive of water if a hydrated crystal is considered.
19. J. F. Charnell, *J. Cryst. Growth.*, **8**, 291 (1971).
20. N. H. Heo, Ph. D. Thesis, University of Hawaii, 1987.
21. K. Seff and M. D. Mellum, *J. Phys. Chem.*, **88**, 3560 (1984).
22. K. Seff, *J. Phys. Chem.*, **76**, 2601 (1972).
23. B. A. Frenz and Y. Okaya, Structure Determination Package Programs, Version 1.2.0(1985), Enraf-Nonius, Delft (Holland).
24. P. A. Doyle and P. S. Turner, *Acta Crystallogr. Sec. A*, **24**, 390 (1968).
25. "International Tables for X-ray Crystallography", Vol. IV, Kynoch Press, Birmingham, England, p. 73, 1974.
26. D. T. Cromer, *Acta Crystallogr.*, **18**, 17 (1965).
27. Reference 25, pp. 149-150.
28. A Discussion of the structure and of the nomenclature

- used for zeolite A is available (a) L. Broussard and D. P. Shoemaker, *J. Am. Chem. Soc.*, **82**, 1041 (1960); (b) K. Seff, *Accounts Chem. Res.*, **9**, 121 (1976).
29. Y. Kim and K. Seff, *Bull. Korean Chem. Soc.*, **8**, 69 (1987).
 30. N. H. Heo, C. Dejsupa, and K. Seff, *J. Phys. Chem.*, **91**, 3943 (1987).
 31. K. Ogawa, M. Nitta, and K. Aomura, *J. Phys. Chem.*, **82**, 1665 (1978).
 32. T. Takahashi and H. Hosoi, *J. Phys. Chem.*, **86**, 2089 (1982).
 33. "Handbook of Chemistry and Physics", 63rd Ed., Chemical Rubber Co., Cleveland Ohio, 1982/1983, PF176.
 34. T. B. Vance, Jr. and K. Seff, *J. Phys. Chem.*, **79**, 2163 (1975).
 35. R. L. Firor and K. Seff, *J. Am. Chem. Soc.*, **99**, 6249 (1977).
 36. V. Subramanian and K. Seff, *J. Phys. Chem.*, **83**, 2166 (1979).

Relation Between the Repulsive Interaction and the Overlap of the Electron Densities[†]

Hoon Heo, Kook Joe Shin, and Yung Sik Kim*

Department of Chemistry, Seoul National University, Seoul 151-742. Received January 9, 1989

The relations between the repulsive interactions and the electron density overlaps are investigated for various closed shell-closed shell pairs, including the systems containing alkali and halide ions. It is found that the repulsive interaction (V_{rep}) depends on the overlap of the electron density (S_o) according to a simple exponential relation, $V_{rep} = AS_o^\alpha$. Furthermore, for most of the closed shell systems the α values are near unity and the A values do not vary much. The same tests are also performed for the open shell-closed shell, and the open shell-open shell pairs. Although the results for these systems also show exponential dependences of the repulsive interactions on the density overlaps, the details of the dependence differ greatly from those for the closed shell systems and also vary widely from one individual system to another.

Introduction

Closed shell repulsive force is generally interpreted in a simple manner in terms of the Pauli exclusion principle: The principle effectively prevents overlapping of the electron densities when they come close to each other, thus leading to higher energy, the cause of the repulsion¹. This in turn suggests that the closed-shell repulsions depend in some way on the overlap of electron densities².

Much work was done to understand the relation between the dominant part of the repulsion, *i.e.* the exchange repulsion, and the overlap of the wavefunctions, densities, or some other related quantities³. The so-called "Mulliken approximation" is an earliest example:

$$E_{ex}(R) = kS^2/R, \quad (1)$$

where S is the overlap integral at internuclear distance R producing the exchange repulsion E_{ex} ⁴. Murrell and Texeira-Dias⁵ proposed an alternative approximation,

$$E_{ex}(R) = (a+bR) \iint \phi_a^2(1) r_{11}^{-1} \phi_b^2(2) dr, \quad (2)$$

where the integral represents the overlap-dependent part of the Coulomb integral.

Several years ago one of the present authors (YSK) and coworkers checked the direct quantitative relationship be-

tween the entire repulsive interaction and the density overlap itself for the closed shell systems⁶. They performed their tests on three inert gas systems, He-He, Ne-Ne and Ar-Ar, and reported a striking result that over most of its repulsive part the interaction is approximately proportional to the overlap of the electron densities (S_o). Their results showed that the rough magnitudes of those closed-shell repulsive interactions depend only on the size of the density overlaps and not on the species of the interacting atoms. At a same interatomic distance the Ar-Ar interaction is more repulsive than the He-He interaction because the Ar system has a larger density overlap than does the He system; but at a same value of the density overlap the repulsive interactions of the two systems do not differ very much. More recently Nyeland and Toennies⁷ used a new quantity

$$N = S_o/R^2, \quad (3)$$

which is the density overlap divided by the square of the internuclear distance, and found that the dependence of the repulsive potentials on N is more stable than the dependence on S_o for wider ranges of R for most of the inert gas systems.

In the present paper we perform the test of Ref. 6 for the closed shell systems that were not tested in the original work. In addition to the inert gas pair systems tested by Nyeland and Toennies in Ref. 7, they also include the systems involving alkali and halide ions. The results exhibit roughly the same trend found in the original work. We also check whether the test can be extended to different types of systems, namely open shell-closed shell systems and the open

[†]This work was supported in part by the Basic Research Institute Program, Ministry of Education of Korea, 1987.